

# Effect of Hexagonal Boron Nitride Nanoparticles Additions on Corrosion Resistance for Zinc Coatings of Weathering Steel in Rainwater

Dhurgham A. Mohsin<sup>1,\*</sup>, Haider M. Lieth<sup>2</sup>, Murtadha A. Jabbar<sup>3</sup>

<sup>1,2,3</sup> Department of Mechanical Engineering, College of Engineering, University of Basrah, Basrah, Iraq

E-mail addresses: [engpg.dhurgham.ali@uobasrah.edu.iq](mailto:engpg.dhurgham.ali@uobasrah.edu.iq), [haider.lieth@uobasrah.edu.iq](mailto:haider.lieth@uobasrah.edu.iq), [murtadha.jabbar@uobasrah.edu.iq](mailto:murtadha.jabbar@uobasrah.edu.iq)

Received: 12 February 2023; Accepted: 6 March 2023; Published: 2 July 2023

## Abstract

Zinc and its alloy coatings are commonly used to provide cathodic protection for weathering steel. However, the steel substrate corrodes faster than the Zinc coating because of the coating's negative corrosion potential. Many studies have examined Zinc and alloy coatings' resistance to corrosion. Hot-dip galvanizing, Electrodeposition, and Zinc-rich coat (ZRC) spray are just some of the methods that can be used to deposit such coatings. Commercially available 99.95 % pure Zinc oxide was used in the electroplating process in this investigation. Steel samples were plated in Zinc sulphate and Zinc oxide solutions and were controlled by different bath parameters such as voltage, current, pH, temperature, and coating time. The addition of hexagonal Boron Nitride (h-BN) nanoparticles has also shown significant improvements in corrosion resistance. However, Zinc-based coating techniques reinforced with h-BN incorporation show the best corrosion current density ( $I_{corr}$ ) of Hot dip 2 % wt. ( $2.1 \mu\text{A}/\text{cm}^2$ ), ZRC 2.5 % wt., ( $4.4 \mu\text{A}/\text{cm}^2$ ), and electroplating 15.75 g/L ( $0.081 \mu\text{A}/\text{cm}^2$ ), which is an order of magnitude lower than coatings without h-BNs. The corrosion rates and current densities of Zn/h-BN coated layers were investigated in a controlled laboratory environment that mimicked natural conditions (Rainwater solution) by extrapolating polarization curves.

**Keywords:** Zinc, Boron Nitride (h-BN) nanoparticle, Corrosion resistance, Cold dip, Hot dip, Electroplating.

© 2023 The Authors. Published by the University of Basrah. Open-access article.

<https://doi.org/10.33971/bjes.23.1.9>

## 1. Introduction

Zinc galvanization has been used extensively in the construction industry, particularly in the weathering steel used in the creation of bridges, buildings, and pipelines due to its exceptional resistance to corrosion.

Cold dip, hot dip, and electro-galvanizing are the three most common methods for producing Zinc-based galvanized steel sheets. There is a close relationship between the coating's microstructure and surface characteristics and its performance [1]. High-temperature oxidation of Zinc-electroplated grey cast iron produced a sub-surface layer with ideal defect distribution and compressibility stresses, greatly improving the material's fatigue and corrosion resistance [2]. Surfaces electroplated with Zinc have microstructural features indicative of a successful deposition process.

Electrodeposition additives (thiourea and dextrin on Zinc electroplating on mild steel in Acid Chloride solution) had a significant impact on the final product, and the plated samples proved more resistant to corrosion in salt water than the uncoated ones [3]. Because of differences in grain size and the incorporation of inert particles, Zinc composites exhibit a slightly more positive corrosion potential and lower corrosion current densities than pure Zinc coatings. Diamond or alumina particle addition to coatings slightly improved their corrosion resistance [4]. As the current density is increased, the weight of all Zinc deposition layers, regardless of their thickness or composition, will increase. Corrosion resistance performance

of Zinc coatings produced by cold spraying versus other processes. Corrosion resistance is enhanced by the corrosion current density ( $I_{corr}$  of  $28.24 \text{ A}/\text{cm}^2$ ) and corrosion potential ( $E_{corr}$  of  $-0.1 \text{ mV}$ ) values calculated from polarization data for up to 72 hours of exposure to a NaCl solution with a pH of 7. An anti-corrosion barrier of at least 72 hours can be maintained by a Zinc cold dip coating applied to a mild steel base. The increased thickness made possible by cold spray makes it a viable option for extending the useful life of sacrificial Zinc coatings [5]. A metallic coating is highly advantageous in situations where preventing corrosion and abrasion is of paramount importance. In addition, electrochemical studies proved that ZRC's corrosion behavior was enhanced by the addition of nanoparticles. Adding nickel-20 chromium nanoparticles to ZRC increased corrosion resistance by 88.7 percentage points, while adding both TiO<sub>2</sub> and nickel-20 chromium nanoparticles increased it by 99.8 percentage points [6]. Both calcium-free alkaline solutions and model pore solutions, (containing Ca<sup>2+</sup>) influenced the corrosion characteristics of hot-dip galvanized steel by varying the pH and the severity of the resulting corrosion attack on the coating. Changes in air pH have a major impact on Zinc corrosion. Zinc corrosion rates were found to be unacceptable in both very alkaline (high pH) and very acidic (low pH) environments. Buildings with galvanized reinforcement last much longer than those without. This coating's benefits include improved resilience in the face of carbonation [7]. Composite coatings that contain h-BN are superior to those

that do not contain h-BN in terms of their ability to withstand corrosive conditions and protect against corrosion. On the manufactured phosphate sample with the heaviest coating mass of  $25 \text{ gm}^{-2}$  and when Boron Nitride nanoparticles were present at about  $0.4 \text{ gL}^{-1}$ , the best anti-corrosion performance was observed ( $I_{corr}$  of  $3.5 \times 10^{-6} \text{ A/cm}^2$  with 325 seconds). This was determined by measuring the current density in a current density meter over a period of 325 seconds. However, the nanoparticles used crystallize phosphate or protect phosphate coatings from corrosion. These nanoparticles have a spherical shape and a very small specific surface area [8]. The objectives and aims of this study are to improve the corrosion resistance of selected Weathering steel using Zinc based coating techniques reinforced by hexagonal Boron Nitride nanoparticles additions. Electrodeposition, Hot dipping, and ZRC will all be used to apply the Zinc coating. The hexagonal Boron Nitride nanoparticles will be added in various percentages and concentrations, and then an optimization process will be carried out to determine the ideal nanoparticle ratios for the best corrosion resistance.

## 2. The Experimental work

### 2.1. Raw material

The chemical composition was measured using a spectrum analyzer (Model SPECTROTEST TXC25) in accordance with ASTM Standard (ASTM 751-14, a) [9]. Table 1 indicates the chemical composition for supplied material Weathering steel grade A588 compared with standard one [10].

After cutting the steel plate to several substrates ( $5 \text{ cm}$  length  $\times$   $5 \text{ cm}$  width  $\times$   $0.4 \text{ cm}$  thickness) in dimensions, cleaning and sandblasting the surfaces in performed in complies with (SSPC/NACE and ISO 5801, 2015), the steel samples were ready for Zinc based coatings [11].

Table 1. Chemical composition for Weathering steel.

Element	Measured value Wt. %	Standard Value % [10]
C	0.1	0.12
Si	0.38	0.298
Mn	0.43	0.36
P	0.101	0.106
S	0.002	0.001
Cr	0.38	0.5
Mo	0.007	0.021
Ni	0.158	0.197
Al	0.42	0.45
Co	0.003	0.006
Cu	0.298	0.249
Ti	0.002	0.004
V	0.004	0.003
W	0.01	> 0.01
Fe	Remainder	Remainder

### 2.2. Boron Nitride (h-BN) nanoparticles characterization and properties

The scanning electron micrograph (SEM) image of h-BNs shown in Fig. 1. The h-BNs found in commercial applications are thin, circular plates with an average thickness of  $65 \text{ nm}$  [8]. Agglomerations of h-BNs can be seen, with extreme stacking

because of the potent Van der Waals interactions. The XRD pattern reveal the phase composition of h-BN. Figure 2 showed prominent characteristic peaks that could be attributed to highly crystallized hexagon h-BNs lying on the (002), (100), (101), (102), (104), and (110) crystallographic planes. The primary apex (highest point) is located at (002). Diffraction  $2\theta = 26.6$  degrees,  $41.5$  degrees,  $43.8$  degrees,  $50.01$  degrees,  $55.1$  degrees,  $73.85$  degrees, and  $75.98$  degrees all showed peaks. Figure 3 shows the results of an EDS analysis performed on h-BN nanoparticles.

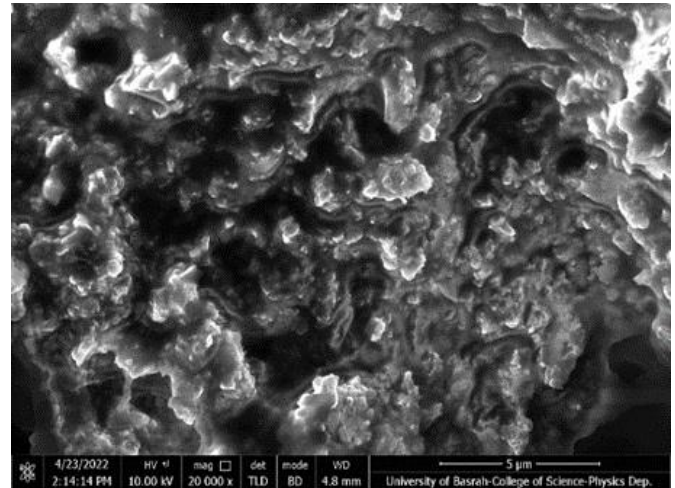


Fig. 1 SEM image of h-BN.

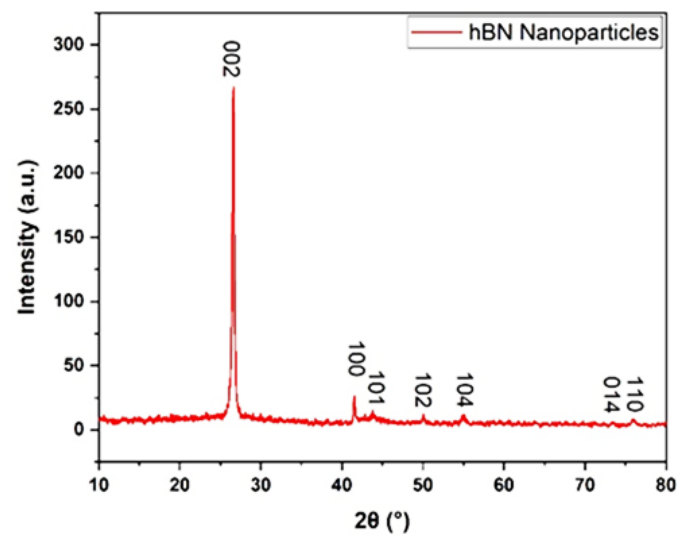


Fig. 2 XRD pattern of h-BN.

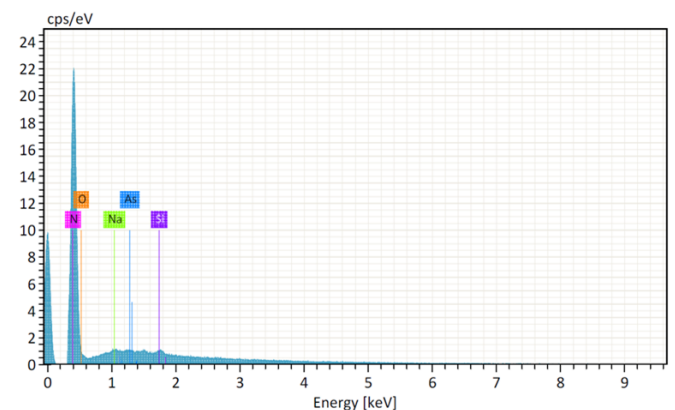


Fig. 3 EDS analysis of h-BN.

### 2.3. Zinc based coating

#### 2.3.1. Zinc electroplating coating reinforced with h-BN nanoparticles.

Electroplating is the method that has been the most popular with consumers and the one that has been utilized the most frequently to deposit a coating on a fastener. It is an electrolytic process, and in order to complete the external circuit, it requires a plating solution, as well as a cathode, and an anode electrode [1]. The electroplating procedure carried out according to the standard specification for Zinc electroplating coatings for iron and steel (ASTM B320) [13]. Electroplating used to apply the Zinc coatings onto the weathering steel substrates. The barrel containing the components to be plated is the cathode, and the plating material is the anode. A wired connection between the cathode and anode forms an external circuit. Positive and negative terminals of the DC power supply are connected to the anode and cathode, respectively. An electrochemical cell is a device in which two electrodes are immersed in an electrolyte, allowing metal ions to move electrochemically from one electrode to the other. Electrons are transferred from the anode, via an external circuit, to the cathode in an oxidation reaction [1]. Besides, reduction occurs at the cathode when metal ions transfer from the anode and/or electrolyte to acquire electrons. The selected steel samples submerged in a Nitric acid solution for 10 minutes to remove oil, organic waste, and surface biosolids, then rinsed three times with deionized water, and finally dried with compressed air. There were three distinct aqueous electroplating baths used to achieve the Zinc electroplating coating process.

Bath A contains 600 g of  $ZnSO_4 \cdot 7H_2O$  dissolved in 2 L of sterile water. To make an ion-free electrolyte, Zinc oxide and pure Sulfuric acid were combined; then, Zinc sulphate at a concentration of 56 g/L was added to a 250 mL beaker (Bath B). When the electrolyte reached 90 °C, 39 g/L of pure Zinc oxide were added and the solution was stirred with a magnetic stirrer at 100 rpm for 20 minutes, during which time the oxide powder had completely dissolved. While leaching, neutralizing, and filtering, the solution maintained at 35 °C and stirred for 20 minutes. The remaining acid was neutralized by adding 1.75 g of pure Zinc oxide in the form of slurry to the solution at a temperature of 35 °C. The electronic scale was used both before and after coating to determine the exact weight of the steel sheets. Zinc discs were used as anodes in the electroplating bath. Before being hung at the cathode of the Zinc electroplating bath, the steel sheet was weighed and secured to the malleable copper wire.

Using a magnetic stirrer, coating procedure experimented with different coating parameters, times (5, 10, 15, and 20 minutes), electric voltages (15, 20, 25, and 30 V). The electrodes spacing selected 3 cm to improve the solution's convection and mass transfer. The pH was kept at 4.5 and the temperature was kept at  $47$  to  $49 \pm 2$  °C. A final rinse with clean water performed and the steel sample was dried at the room temperature for five minutes, then the Zinc-coated steel sample reweighed again.

The h-BN nanoparticles in (Bath C) were analyzed using SEM and found to have a mean particle size of 63 nm and a purity of 99.99 %. The h-BNs nanoparticles provided from Luoyang Tongrun Info Technology Co., Ltd., a division of Alibaba Industrial Corporation. The h-BN nanoparticles were added to the Zinc electroplating process at four different concentrations: h-BN-5.25, h-BN-10.5, h-BN-15.75, and

h-BN-21 g/l. After the solution mechanically stirred for 4 hours, the Zinc electroplating solution was sonicated using a Sonicator machine with a fixed shelf (Sonicator was supplied from Hangzhou Precision Machinery Co., Ltd., Ali Express Industrial corporation, China) for 2 hours at  $56 \pm 4$  °C to extract and improve the dispersibility of the h-BNs nanoparticles. A magnetic stirrer was then used to stir up the electroplating bath at a rate of 250 rpm, while keeping the temperature and pH at  $56 \pm 4$  °C and 4.5 to 5, respectively, to ensure that the h-BNs were uniformly dispersed throughout the solution. The Zinc electroplating bath chemical composition and concentrations are listed in Table 2.

**Table 2.** The composition and concentration of the Zinc electroplating baths.

Bath	$ZnSO_4 \cdot 7H_2O$ (gL <sup>-1</sup> )	$H_2SO_4$ (gL <sup>-1</sup> )	ZnO (gL <sup>-1</sup> )	h-BN nanoparticles (gL <sup>-1</sup> )
A	300	-	-	-
B	65	200	39	-
C	65	200	39	5.25 – 10.5 – 15.75 – 21

#### 2.3.2. Zinc dry Hot-dip galvanizing

Dry hot-dip galvanizing conforms to the A53/A53M standard [14]. Before being immersed in a bath of molten Zinc, the prepared steel samples are sandblasted and cleaned with Nitric acid. The ideal temperature for a bath is slightly (by about 10 percent) higher than the melting point of Zinc. As flux,  $ZnCl_2$  and  $NH_4Cl$  salt additives have been used. A hot plate stirrer used and set to 60 °C to flux bath water-washed steel samples in a flux solution (95 g/L  $ZnCl_2$  plus 150 g/L ammonium chloride) for 4 minutes. The flux-coated samples were then galvanized in a molten Zinc bath at  $435 \pm 5$  °C for 90 seconds using Zinc with a purity of at least 99.99 % purchased locally, before being dried in an electrical furnace model thermo (the US-made) at 120 °C for 100 seconds. As the Zinc kettle is shifted along its length, the ash is skimmed off the top. Zinc melt kept in contact with the components constantly at a steep immersion angular position. Parts must remain in the Zinc melt until the flux has boiled off or the temperature has stabilized. Components are cooled rapidly in clean water or after being taken out of the Zinc bath to prevent the formation of white rust [15]. To reinforce the material, hexagonal boron nitride (h-BN) nano powder was incorporated.

In 0.5 wt. % increments, the amount of h-BN nano reinforcement was increased from 0 to 2.5 % as shown in Table 3. Two hours were spent stirring the pure Zinc melt at temperatures between 650 °C and 700 °C, after which flux was introduced to enhance the wettability of the reinforcements. Hexagonal boron nitride (h-BN) was prepared for use in liquid metal by heating it to 450 °C for 30 minutes, which removed organic contaminants and moisture. The mixture was mechanically agitated at vertex formation speed for 20 minutes after the addition of the liquid metal bath (350-400 rpm). The addition of nanoparticles to the melting Zinc alloy caused an immediate increase in the viscosity of the melt. For the sonication process to be successful, the crucible had to be kept at a melting temperature of 800 °C, and the nanoparticles' flowability in a liquid had to be enhanced to decrease its viscosity. Following this, a titanium alloy probe with a processing capacity of 100-2500 mL was subjected to

cavitation using ultrasonic power of 1.0 kW and 20 kHz for 10 minutes while 3/4 of the probe was submerged in a molten Zinc bath. For the next 5 minutes, the bath was mechanically stirred to further disperse the sonicated reinforcement nanoparticle clusters and agglomerates. After being heated to 500 °C, the liquid was either left in the container for 24 hours at room temperature or cooled quickly with clean water.

**Table 3.** Dry hot dip galvanization mixing weights for coating samples.

Sample No.	Additives wt %	Weight (grams)	Total weight (grams)
1	--	100 Pure (Zinc)	100
2	h-BN 0.5 %	2 (h-BN) + 98 (Zinc)	100
3	h-BN 0.1 %	4 (h-BN) + 96 (Zinc)	100
4	h-BN 1.5 %	6 (h-BN) + 94 (Zinc)	100
5	h-BN 2 %	8 (h-BN) + 92 (Zinc)	100
6	h-BN 2.5 %	10 (h-BN) + 90 (Zinc)	100

### 2.3.3. Cold dip - Zinc rich coating (ZRC)

The Zinc rich coat (ZRC) method is governed in accordance to the standard ASTM D520 Type II ASTM,2012 [14]. For cathodic protection, weathering steel typically painted with a Zinc-rich coating (ZRC), typically a grey compound coating and full galvanized system named (ZINCA) [16] provided from local markets. The dry film of cold galvanization is 96 % pure Zinc dust, making it an extremely effective barrier coating, in addition to having the galvanic properties of a Zinc coating. Zinc dust pigment is encased in a binder of epoxy resin and aromatic hydrocarbon, providing better cathodic protection to steel substrate. The physicochemical characteristics of the cold galvanizing compound ZINCA are tabulated in Table 4.

The methods used to apply a ZRC coating are risk-free and easy to manage. This coating system can be applied by brushing, spraying, or even total immersion and does not require any additional tools for application. Procedures utilizing galvanized film industrial cold galvanizing of the highest quality and performance is the best defense against corrosion for any ferrous metal. The steel samples are polished using sandblasting and Nitric acid. At room temperature, 10 mL of thinner were added to every 250 mL of Zinc, and the mixture was stirred for 10 minutes. Zinc paint is sprayed onto a steel surface using compressed air at a constant painting concentration but varying coat numbers (2-4-6-8). Liquid Zinc is then pumped into the spray gun.

**Table 4.** Physical and chemical properties of the cold galvanizing compound-ZINGA [16].

Properties	Values
Zinc Content	96 %
Zinc Purity Degree	99.995 % (minimum)
Density	2.7 kg/dm <sup>3</sup>
Dry Extract	80.3 % by weight
Temperature Resistance	-400 °C to +1500 °C
Drying Time	5 to 10 minutes.
Spreading Rate	40 microns: 4 m <sup>2</sup> / kg
Flash Point	470 °C

Table 5 presents the outcomes that occurred after varying the amount of h-BN nanoparticles that were added. Sonication of the ZINCA paint was performed at room temperature for a period of thirty minutes while the paint was being mixed with thinner (10 mL for every 250 mL of Zinc). After the Zinc has been inserted into a high-pressure air pistol with a nozzle that has a diameter of 2 mm and pressurized to a pressure of 5 bars, it is then sprayed onto a steel surface with compressed air at a specific distance and at specific time intervals for each coat. This is repeated with the same number of squeezing sprays but with h-BN nano concentrations varying in increments of 0.5 weight % from 0 to 2.5 weight %, and then kept drying in the laboratory at a temperature of 30 ± 1 degrees Celsius or by being exposed to direct sunlight for 15 to 30 minutes.

**Table 5.** Zinc-rich coating (ZRC) mixing weights for coating samples.

Sample No.	Additives wt %	Weight (grams)	Total weight (grams)
1	--	100 Pure (Zinc)	100
2	h-BN 0.5 %	5 (h-BN) + 95 (Zinc)	100
3	h-BN 0.1 %	10 (h-BN) + 90 (Zinc)	100
4	h-BN 1.5 %	15 (h-BN) + 85 (Zinc)	100
5	h-BN 2 %	20 (h-BN) + 80 (Zinc)	100
6	h-BN 2.5 %	25 (h-BN) + 75 (Zinc)	100

### 2.4. Corrosion test

On each coated sample, open circuit potential (OCP) was measured, and linear potentiodynamic polarization tests carried out in order to evaluate the coated material's resistance to corrosion as required by ASTM G5-14 [16] and ASTM G1-3 [17]. The tests were carried out at room temperature using a rainwater solution contained within a beaker holding 250 mL. These tests were carried out using a potentiostat of type MLab that was connected to a computer. The potentiostat was comprised of a cell that was outfitted with three different electrodes which was exposed to 1 cm<sup>2</sup> area between the three electrodes. During the initial phase of the testing process, open circuit potential was initially recorded for up to 300 seconds of immersion time. After that, a polarization test was performed, and throughout all the analyses, the scan rate remained constant at 0.001 v/s. After that, Tafel lines were produced with the help of the MLab software to obtain anodic and cathodic slopes, which were subsequently utilized in the computation of ( $E_{corr}$ ), ( $I_{corr}$ ), polarization resistance  $R_p$ , and corrosion rate.

Calculating the rate of uniform corrosion can be done in one of two ways: either automatically using the software that performs corrosion tests after inserting the required calculation parameters, or manually using the equation developed by Faraday [19]:

$$W = \frac{ItM}{nF} = \frac{iAtM}{nF} \quad (1)$$

Where:

$W$ : Weight of metal (g), corroded or electroplated in an aqueous solution in time (s).

$I$ : Current flow (A).

$i$ : Current density (A/cm<sup>2</sup>).

$t$ : Time (s).

$M$ : Atomic mass of metal (g/mol).

$n$ : Number of atoms/electrons produced or consumed.

$A$ : Area ( $\text{cm}^2$ ).

$F$ : Faraday's constant = 96500.

$$\text{Corrosion rate} = 327 \times \frac{I_{\text{corr}} M}{V D A} \quad (2)$$

Considering that one year is equal to 96500 seconds and that one coulomb is equal to one coulomb, we get 327 seconds for one year. The corrosion current density, also known as ( $I_{\text{corr}}$ ) can be determined by locating the point where the linear portions of the anodic and cathodic Tafel curves intersect. In this equation,  $M$  represents the atomic mass,  $V$  represents the number of electrons lost in the oxidation reaction,  $D$  represents the density, and  $A$  represents the exposed area of the sample [20].

### 3. Results and discussion

#### 3.1. Corrosion analysis

##### 3.1.1. Open circuit potential (OCP) test

The OCP is a corrosion-related parameter that characterizes a material's susceptibility to electrochemical oxidation. OCP measurements have proven to be a useful tool for predicting how a material will perform in a polarization test before the polarization test has even begun. Based on the results thus far, we can conclude the following about the material's corrosion behavior. Adding more h-BN to Zinc-based coatings raised their potentials (i.e., increased corrosion resistance). Figs. 4, 5, and 6 shows the open circuit potential changes as a function of running time (300 s) for both the control (uncoated) and Zinc based coated samples in rainwater. The scan rate maintained at 0.001 v/s and a sensitivity of ( $1 \times 10^{-3}$  A/V).

Pure Zinc and Zinc alloys provide significantly better protection against corrosion on the substrate than the control (uncoated) weathering steel. Moreover, the Zinc based coatings strengthened by incorporating the h-BN nanoparticles into the structure have significantly improved corrosion resistance over Zinc alloys and pure Zinc. There was an initial positive shift in the corrosion potential because of adding h-BN nanoparticles to the bath for Zinc electroplating and Hot dip galvanizing (h-BN 15.75 g/L) for electroplating and (h-BN 2 %) for hot dip galvanizing, but this was followed by a shift to the negative side and a gradual increase in ZRC up to (h-BN 2 %).

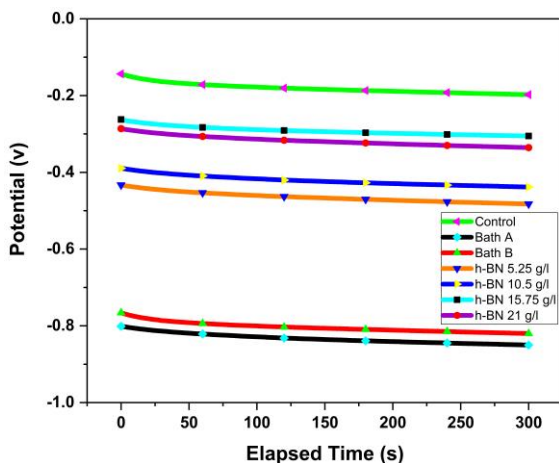


Fig. 4 OCP variation Vs elapsed time for Zinc electroplating coated samples in rainwater.

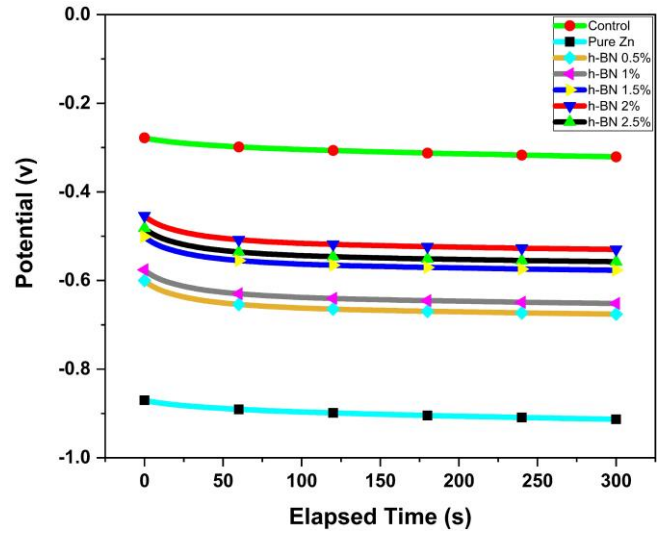


Fig. 5 OCP variation Vs elapsed time for Zinc hot dip coated samples in rainwater.

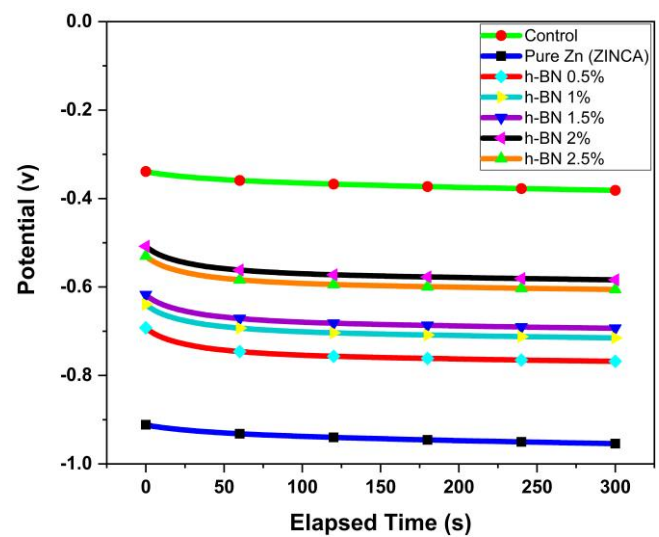


Fig. 6 OCP variation Vs elapsed time for Zinc cold dip coated samples in rainwater.

All overboard of h-BN bath concentrations, Zn/h-BN coatings were found to have higher corrosion potential values than pure Zinc and Zinc alloy coatings. Initially starting at -152 mV, the uncoated (control) sample decreased to -297 mV by the end of the experiment. Electroplating coating galvanizing, when compared to hot dip and ZRC coatings, showed better corrosion improvements. The addition of h-BN bath concentration (15.75 g/L) to electroplating caused the potential to change to a more positive value, with hot dip 2 % (-413 mV to -486 mV) and ZRC 2 % exhibiting potential ranges of (-501 mV to -549 mV). The coating with the highest corrosion potential was created in a bath containing 15.75 g/L h-BN nanoparticles. The following h-BN bath volumes at which electroplating is advised are 10.5, 21, and 5.25 g/L. In terms of corrosion potential, ZRC achieved a best h-BN value of 2.5 %, while hot-dip galvanizing achieved a best h-BN value of 2 %. Therefore, we can conclude that the corrosion performance of h-BN co-deposition with the coating matrix has been improved. As a passive physical barrier, h-BN particles shield the coating from further corrosion deterioration [21]. Sensitized specimens' corrosion behavior (measured by weight loss) was consistent across all corrosive media, with mass loss per area rising with longer ageing times and higher

temperatures. AISI 204 stainless steel becomes less passive as it ages for longer periods of time. Additionally, ( $I_{corr}$ ) increased with age and temperature while ( $E_{corr}$ ) decreased. The  $M_{23}C_6$  carbide precipitation in AISI 204 stainless steel decreased the material's resistance to corrosion when it was subjected to higher temperatures and longer ageing times [22].

### 3.1.2. Potentiodynamic polarization test

Tafel curves of pure Zinc, Zinc alloy coatings, and uncoated (control) weathering steel sample values extracted via extrapolation in rainwater solution are shown in Figs. 7, 8, and 9, as are the polarization behaviors of Zn/h-BN coatings with different h-BN nanoparticle bath concentrations. When the material has a higher corrosion potential, it is more resistant to the effects of corrosion. Corrosion potential ( $E_{corr}$ ), corrosion current density ( $I_{corr}$ ), corrosion resistance ( $R_p$ ), and corrosion rate ( $CR$ ) are some of the electrochemical parameters were displayed in Table 6 from the Tafel extrapolation of polarization curves. Electroplating a Zn/h-BN coating resulted in the best corrosion resistance, especially when the bath concentration of h-BN nanoparticles was 15.75 g/L. Among all h-BN additives, the coated sample with a concentration of 5.25 g/L h-BN in the bath had the poorest ( $E_{corr}$ ), the worst negative side. Coating samples enhanced with h-BN nanoparticles had higher corrosion potentials than those of pure Zinc, Zinc alloy coating, and weathering steel substrate. In addition, the corrosion resistance of pure Zinc and Zinc alloy is higher than weathering steel substrate. In addition, 2 % concentration of h-BN for hot-dip galvanization and a 2.5 % concentration for ZRC yielded the best corrosion potential ( $E_{corr}$ ). Nanomaterial incorporation into Zinc-based coatings results in a non-trivial swing in the corrosion potential ( $E_{corr}$ ) value of the coated samples. It has been argued that the corrosion current density is more essential than the corrosion potential in determining corrosion resistance, since it is directly related to the corrosion rate according to Faraday's law [23]. With an ( $I_{corr}$ ) of ( $0.081 \mu A/cm^2$ ) for electroplating, ( $2.1 \mu A/cm^2$ ) for hot dip, and ( $4.4 \mu A/cm^2$ ) for ZRC, Zn/h-BN coatings with a 15.75 g/L h-BN bath concentration offered the highest corrosion resistance. The recommended concentrations in the bath are then 10.5, 21, and 5.25 g/L, respectively. When considering corrosion resistance, a particle concentration of 15.75 g/L is optimal. In accordance with the densities of the currents that cause the least corrosion. However, when a specific concentration of h-BN nanoparticles was reached, corrosion resistance began to decline. The presence of h-BN particles in the electrolyte prevents hydrogen reactions from occurring on the cathode's surface and reduces the cathode's active surface area [24].

The anodic and cathodic electrochemical processes affected by the incorporation of h-BN particles into a Zinc alloy matrix. These results show that both the cathodic hydrogen production events and the anodic dissolution reactions are evolving. Corrosion resistance may be improved thanks to the ability of h-BN particles to fill micron-sized pores and spaces in the coating's surface [25]. Electroplating a coating with reinforcement particles that distributed at the grain boundaries may improve its compactness and impermeability, hence increasing its resistance to corrosion. As a consequence, corrosion resistance is enhanced [26]. The incorporation of h-BN nanoparticles significantly enhances the electrochemical anticorrosion performance of Zinc-based coatings.

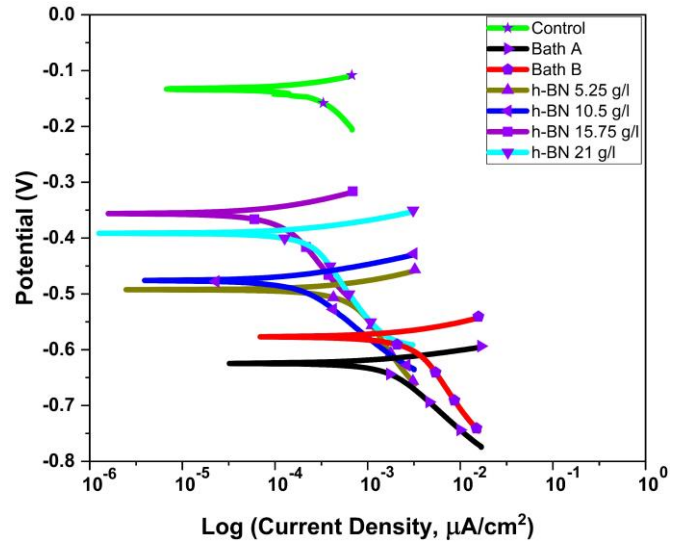


Fig. 7 Potentiodynamic polarization curves of the Zinc electroplating coated samples evaluated in rainwater.

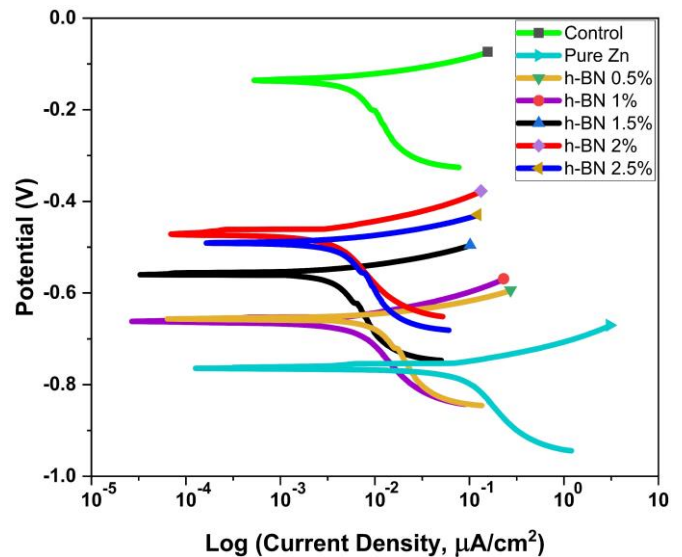


Fig. 8 Potentiodynamic polarization curves of the Zinc hot dip coated samples evaluated in rainwater.

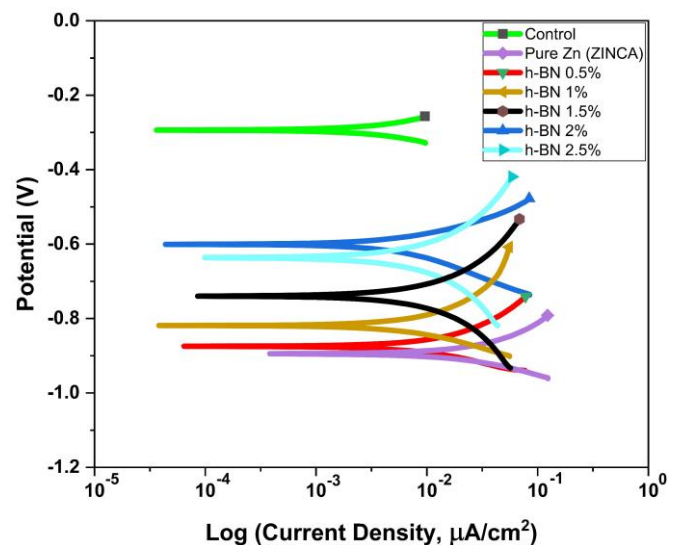


Fig. 9 Potentiodynamic polarization curves of the Zinc cold dip coated samples evaluated in rainwater.

**Table 6.** Corrosion analysis (rainwater solution) of coated specimens.

Coating Sample	$E_{corr}$ (mV)	$I_{corr}$ ( $\mu\text{A}/\text{cm}^2$ )	$R_p$ ( $\Omega \cdot \text{cm}^2$ )	CR (mmpy)
Control (Uncoated)	-143	0.43	4883.72	0.00393
Electroplating Bath A	-627	1.3	1615.38	0.01189
Electroplating Bath B	-579	2.6	807.69	0.0238
Electroplating BN 5.25 g/L	-494	0.59	3559.32	0.00539
Electroplating BN 10.5 g/L	-477	0.17	12352.94	0.00155
Electroplating BN 15.75 g/L	-357	0.081	25925.92	0.00074
Electroplating BN 21 g/L	-394	0.26	8076.93	0.00238
Control (Uncoated)	-124	8.2	256.09	0.07505
Hot dip Pure Zinc	-965	24.4	86.06	0.22333
Hot dip h-BN 0.5 %	-661	7.4	283.78	0.06773
Hot dip h-BN 1 %	-666	5.8	362.06	0.05307
Hot dip h-BN 1.5 %	-561	4.9	428.57	0.04484
Hot dip h-BN 2 %	-469	2.1	1126.23	0.01922
Hot dip h-BN 2.5 %	-494	2.9	724.13	0.02654
Control (Uncoated)	-292	5.9	355.93	0.05398
ZRC ZINCA	-889	21	101.02	0.19221
ZRC h-BN 0.5 %	-872	8.2	256.09	0.07505
ZRC h-BN 1 %	-819	5.4	388.88	0.04941
ZRC h-BN 1.5 %	-739	5.1	411.76	0.04667
ZRC h-BN 2 %	-592	5	423.23	0.04575
ZRC h-BN 2.5 %	-628	4.4	487.72	0.04027

#### 4. Conclusions

The hot-dip, ZRC, and traditional electrodeposition techniques used to plate Zn/h-BN composite coatings. The results reveal that Zinc alloy coatings effectively coated with h-BN first phase particles resulted in compact, smooth surfaces and fine-grained crystal structures in the composite coatings. Corrosion resistance improved at a certain concentration of h-BN particles. Incorporating h-BN nanoparticles has the potential to reduce porosity and improve grain quality due to their role as nucleation sites. One major finding from studies on corrosion is that the addition of h-BN particles to a Zinc alloy coating greatly improves the coating's ability to resist corrosion.

The corrosion resistance of composite coatings made in h-BN baths of varying concentrations has been shown to be superior to that of pure Zinc and Zinc alloy coatings. The best corrosion resistance was shown by the composite coating produced in a bath containing (Electroplating) 15.75 g/L, (Hot dip) 2 wt %, and (ZRC) 2.5 wt % h-BN concentration. As an additive, h-BN nanoparticles show the highest anticorrosion performance against copper sulphate dropping corrosive for electroplating ( $0.081 \mu\text{A}/\text{cm}^2$ ), hot dip ( $2.1 \mu\text{A}/\text{cm}^2$ ), and ZRC ( $4.4 \mu\text{A}/\text{cm}^2$ ), respectively.

#### References

- [1] P. P. Chung, J. Wang, and Y. Durandet, "Deposition processes and properties of coatings on steel fasteners-A review", *Friction*, Vol. 7, Issue 5, pp. 389-416, 2019. <https://doi.org/10.1007/s40544-019-0304-4>
- [2] A. S. Hammood and H. M. lieth, "Development artificial neural network model to study the influence of oxidation process and zinc-electroplating on fatigue life of gray cast iron", *International Journal of Mechanical and Mechatronics Engineering*, Vol. 12, Issue 5, pp. 128-136, 2012.
- [3] C. A. Loto and R. T. Loto, "Effect of dextrin and thiourea additives on the zinc electroplated mild steel in acid chloride solution", *International Journal of Electrochemical Science*, Vol. 8, Issue 12, pp. 12434-12450, 2013.
- [4] I.-D. Utu, R. Muntean, and I. Mitelea, "Corrosion and Wear Properties of Zn-Based Composite Coatings", *Journal of Materials Engineering and Performance*, Vol. 29, Issue 8, pp. 5360-5365, 2020. <https://doi.org/10.1007/s11665-020-04995-4>
- [5] N. M. Chavan, B. Kiran, A. Jyothirmayi, P. S. Phani, and G. Sundararajan, "The corrosion behavior of cold sprayed zinc coatings on mild steel substrate", *Journal of thermal spray technology*, Vol. 22, Issue 4, pp. 463-470, 2013. <https://doi.org/10.1007/s11666-013-9893-z>
- [6] M. A. Jabbar, A. D. Hassan, and Z. A. Hamza, "Organic zinc-rich protective coatings with improved electrochemical properties: The role of nano-powder additions", *Cogent Engineering*, Vol. 8, Issue 1, 2021. <https://doi.org/10.1080/23311916.2020.1870793>
- [7] P. Pokorný, P. Tej, and M. Kouřil, "Evaluation of the impact of corrosion of hot-dip galvanized reinforcement on bond strength with concrete-a review", *Construction and Building Materials*, Vol. 132, pp. 271-289, 2017. <https://doi.org/10.1016/j.conbuildmat.2016.11.096>
- [8] H. Huang, H. Wang, Y. Xie, D. Dong, X. Jiang, and X. Zhang, "Incorporation of boron nitride nanosheets in zinc phosphate coatings on mild steel to enhance corrosion resistance", *Surface and Coatings Technology*, Vol. 374, pp. 935-943, 2019. <https://doi.org/10.1016/j.surfcoat.2019.06.082>
- [9] ASTM A751-14, "Standard Test Methods, Practices and Terminology for Chemical Analysis of Steel Products", ed: ASTM International West Conshohocken, PA, 2014.
- [10] A. K. Ray, B. Goswami, A. Raj, M. J. J. o. M. Singh, and M. Science, "High strength low alloy steels", Vol. 55, Issue 1, pp. 21-36, 2013.
- [11] R. Francis, "Surfaces, Standards and Semantics: A Close Look at Visual Surface Cleaning Standards", *Journal of Protective Coatings and Linings*, Vol. 32, Issue 2, pp. 27-30, 2015.
- [12] A. Brenner, *Electrodeposition of alloys: principles and practice*, Elsevier, 2013.
- [13] ASTM A53/A53M-12, "Standard Specification for Pipe, Steel, Black and Hot-Dipped, Zinc-Coated, Welded and Seamless", ASTM International Standard, 2012.
- [14] Y. Wang, G. Liang, J. Long, and X. Feng, "Enhanced Corrosion Resistance of hot-dip Galvanized Zinc Coating on AZ31 Magnesium Alloy with Cu Interlayer", *International Journal of Electrochemical Science*, Vol. 17, No. 220531, pp. 1-13, 2022. <https://doi.org/10.20964/2022.05.20>

- [15] M. T. Islam and M. A. Chowdhury, "Surface corrosion of mild steel structures", Proceedings of the International Conference on Mechanical Engineering 2003 (ICME2003), Dhaka, Bangladesh, 26-28 December 2003.
- [16] ASTM G5-14, "Standard Reference Test Method for Making Potentiodynamic Anodic Polarization Measurements", ASTM International Standard, 2014.
- [17] ASTM G1-3, "Standard practice for preparing, cleaning, and evaluating corrosion testing specimens", ASTM International Standard, 2011.
- [18] ASTM G102-89, "Standard practice for calculation of corrosion rates and related information from electrochemical measurements", ASTM International Standard, 2010.
- [19] M. Cui, C. Xu, Y. Shen, H. Tian, H. Feng, and J. Li, "Electrospinning superhydrophobic nanofibrous poly (vinylidene fluoride)/stearic acid coatings with excellent corrosion resistance", *Thin Solid Films*, Vol. 657, pp. 88-94, 2018. <https://doi.org/10.1016/j.tsf.2018.05.008>
- [20] S. Paydar, A. Jafari, M. E. Bahrololoom, V. Mozafari, "Influence of BN and B<sub>4</sub>C particulates on wear and corrosion resistance of electroplated nickel matrix composite coatings", *Tribology - Materials, Surfaces & Interfaces*, Vol. 9, Issue 2, pp. 105-110, 2015. <https://doi.org/10.1179/1751584X15Y.0000000007>
- [21] M. J. Joseph and M. A. Jabbar, "Effect of aging process on the microstructure, corrosion resistance and mechanical properties of stainless steel AISI 204", Vol. 11, No. e00253, 2019. <https://doi.org/10.1016/j.cscm.2019.e00253>
- [22] ASTM G102-89, "Standard practice for calculation of corrosion rates and related information from electrochemical measurements", ASTM International Standard, 2010.
- [23] E. Ünal, and İ. H. Karahan, "Production and characterization of electrodeposited Ni-B/hBN composite coatings", *Surface and Coatings Technology*, Vol. 333, pp. 125-137, 2018. <https://doi.org/10.1016/j.surfcoat.2017.11.016>
- [24] S. Kasturibai, and G. P. Kalaignan, "Characterizations of electrodeposited Ni-CeO<sub>2</sub> nanocomposite coatings", *Materials Chemistry and Physics*, Vol. 147, Issue 3, pp. 1042-1048, 2014.
- [25] Y. Wang, Sh.-J. Wang, X. Shu, W. Gao, W. Lu, and B Yan, "Preparation and property of sol-enhanced Ni-B-TiO<sub>2</sub> nano-composite coatings", *Journal of Alloys and Compounds*, Vol. 617, pp. 472-478, 2014. <https://doi.org/10.1016/j.jallcom.2014.08.060>